17th International Symposium on Ice
Saint Petersburg, Russia, 21 - 25 June 2004
International Association of Hydraulic Engineering and Research

Session I

SOME RESULTS OF 3D NUMERICAL SIMULATION OF LEVEL ICE-STRUCTURE INTERACTION

K.N. Shkhinek[1], A.G. Jilenkov[1], S.M. Kapustiansky[1], T. Kärnä[2] and S. Løset[3]

ABSTRACT

This paper presents some results of a 3D numerical simulation model for level ice-structure interaction. The method of solution uses the Wilkins' (1973) finite-difference methodology and described by Jilenkov et al. (2002). The analyses in that paper showed that the Drucker-Prager failure criterion gives results close to a modified Coulomb-Mohr criterion but needs less of computations because in this criterion we should not determine principle stresses in any point for each time step. This criterion is used in this paper. Some results of computations, namely velocity effect, stress distribution along the contact surface, problems of non-simultaneous failure are discussed.

INTRODUCTION

 The problem of ice sheet/vertical structure interaction was considered by Kärnä (1995), Shkhinek et al. (1999) and Kärnä et al. (2001). However, all these studies examined only 2D solutions either in the level ice plane or normal to it. Kärnä et al. (2001) tried to include some corrections to the 2D solution in order to achieve an approximation of the 3D phenomena, but this result was based on several assumptions. Most of these assumptions have a physical background, but some coefficients were not well founded. The 3D numerical solution was published by Jilenkov et al. (2003). This method is based on the finite-difference method. The Wilkins' (1973) methodology is used in the present work

The selection of relevant failure criterion is quite important in theoretical solutions. Comparison of results of computations corresponding to different 3D criteria (modified Coulomb-Mohr, Drucker-Prager, and Schulson [11, 12] showed that the difference in results predicted by different criteria is not very great. Therefore the simplest Drucker-Prager was used for wide experiments.

---

[1] St. Petersburg Technical University, Russia
[2] VTT Building and Transport, Finland
[3] Norwegian University of Science and Technology, Norway

STATEMENT OF THE PROBLEM

Assume an infinite ice sheet with thickness h that moves with velocity U_∞ against a structure (vertical, immovable, absolutely rigid wall) of width L (Fig. 1). The ice sheet covers the surface described by $X > 0, -\infty < Y < \infty$. As the structure has a limited width and the ice a limited thickness, the phenomena should be considered as 3D. It is assumed that the sheet hits the wall at time $t = 0$. The task is to consider characteristic of the stress/strain field in the 3D solution and to compare the calculation results with some experimental data.

THE CONSTITUTIVE EQUATIONS

Two systems of coordinates are used in the computations. The global one (X,Y,Z) is related to the entire ice field. The local system is related to the elements that represent parts of the ice field. Let us assume that ice failure may develop both by shear and by tension.
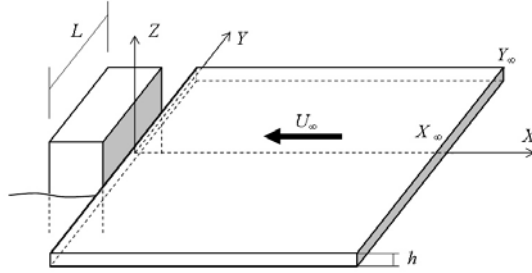

Fig. 1. Sketch of the computational set-up

It is assumed that the elastic-plastic model describes the failure of this type. It proposed also that the ice velocity is sufficiently high and creep does not exist. Initially the material is considered as elastic. As soon as the failure criterion is reached in any point of the material, the ice properties in such a point is set to a residual state with a reduced strength. The main equations for the 3D phenomenon may be written in the following form ($i, j = 1, 2, 3$):

$$\rho V = \rho_0 V_0 \tag{1a}$$

$$\rho \frac{dU_i}{dt} = \frac{\partial S_{ij}}{\partial x_j} - \frac{\partial P}{\partial x_i} \tag{1b}$$

$$\frac{DS_{ij}}{Dt} = 2G\left(e_{ij} - \frac{1}{3}e_{kk}\delta_{ij} - \dot{\lambda}S_{ij}\right) \tag{1c}$$

$$\frac{dP}{dt} = -K\left(e_{kk} - 2\Lambda\dot{\lambda}\tau\right). \tag{1d}$$

Summation is made over the recurring indices and the following notation is used: $x_1 \equiv X$, $x_2 \equiv Y$, $x_3 \equiv Z$. ρ, ρ_0 and V, V_0 are the ice densities and volume in the current and the initial states, respectively. U_i is the projection of the velocity vector on the x_i-axis of the global system of coordinates and t is time. Moduli G and K are the shear and bulk modulus, $\frac{D}{Dt}$ is the Jaumanns derivative, $e_{ij} = \frac{1}{2}\left(\frac{\partial U_i}{\partial x_j} + \frac{\partial U_j}{\partial x_i}\right)$ are the components of the tensor of the velocity of deformation, and Λ is the velocity of

dilatancy (assumed equal to zero in the numerical experiments). The intensity of the shear stress is $\tau^2 = \dfrac{3}{8} S_{ij} S_{ij}$ and $\dot{\lambda}$ is the factor to be determined from the conditions that stresses reach on the ultimate strength surface (otherwise $\dot{\lambda} = 0$). The components of the stress tensor are considered as a sum of the components of the spherical stress tensor and the deviatoric stress tensor in the form $\sigma_{ij} = -P\delta_{ij} + S_{ij}$ where $P = -\sigma_{kk}/3$ is the hydrostatic pressure, S_{ij} components of the tensor deviator and δ_{ij} is the Kroneker's delta. The modified Coulomb-Mohr criterion is used in the form suggested by Drucker-Prager. It takes into account the strength dependence on invariants:

$$\sqrt{3I_2} = Y_1 + Y_2 P, \tag{2}$$

where $I_2 = ((\sigma_1 - \sigma_2)^2 + (\sigma_2 - \sigma_3)^2 + (\sigma_3 - \sigma_1)^2)/6$ is the ultimate value of the second invariant of the deviatoric stress tensor, and

$$Y_2 = 3(tg^2\alpha - 1)/(tg^2\alpha + 2), \; Y_1 = R_c(1 - Y_2/3), \; \alpha = 45^0 + \varphi/2, \tag{3}$$

are some functions. R_c is the uniaxial compressive strength of ice and φ is the angle of internal friction. If the failure criterion is reached in some cell, the ice strength is set to the residual value. The criterion of the tensile failure was used in the form $P = -\sigma_t/3$. As soon as the criterion of the tensile failure is reached, the maximum principle tensile stress is assumed to be zero in this point.

Initial and boundary conditions
Initial conditions:
The initial conditions are as follows:

$$U_X = U_\infty, U_Y = U_Z = 0, \sigma_{ij} = 0 \tag{4}$$

Boundary conditions
Sliding conditions without friction are used in the present solution, but the model allows the use of any other conditions. As the real infinite area of the ice sheet cannot be considered, only the quasi-infinite area is investigated. This means that we exclude any wave reflection from boundary surfaces located at $X = X_\infty, Y = Y_\infty$. This condition can be written in the form suggested by Lysmer and Kuhlemeuer, 1969.

The computational algorithm
The Lagrangian finite difference net was used for the integration of the equations. The volume of ice was divided into cells. These cells do not overlap each other and there are no gaps between them. The apexes of the cells are the nodes of the net. The hexahedron cells that were used in the Wilkins' method [14] were additionally divided into tetrahedron elements (Fig. 2). The components of the velocity are referred to the nodes of the net at the time that corresponds to the half time step ($t + \Delta t/2$). The ice density and the components of the tensors of strain rates and stresses are referred to the cell centre and determined at the time corresponding to the whole time step ($t + \Delta t$).
The finite-difference scheme for integration of the system of equations can be obtained as a result of replacing the partial derivatives in space by integrals along the contour
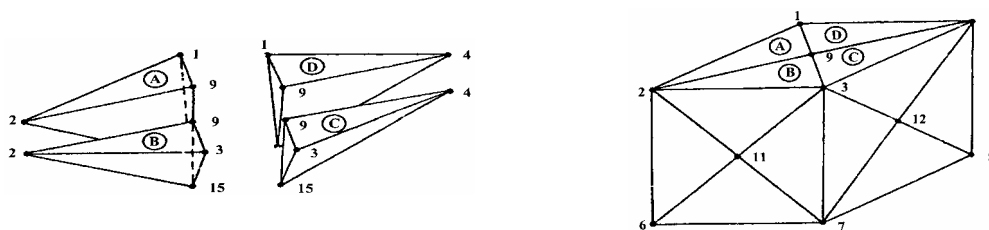
Fig. 2. The cells for computation. The hexahedron cell and its division into tetrahedron elements

of the corresponding elements and use of the theorem about the mean value. The time derivatives are approximated by the central differences. More detailed description of the methodology can be found by Jilenkov et al. (2003).

SOME RESULTS FROM THE NUMERICAL EXPERIMENTS

Parameters used in experiments

The following parameters were used in numerical experiments (if it does not specified specially): the structure length L- 5, 10.20 and 40m; the ice thickness h-0.5,1, 2 and 4m.,the ice velocity V- 0.1, 0.5 and 1m/s, modulus of deformation- E=9GPa, unconfined strength-R_c-1MPa, residual strength R_r-0.25R_c and 0.95R_c, tensile strength $R_t = 0.2\,R_c$, Poisson coefficient –0.3, angle of internal friction φ -25° and 85°.

Influence of ice velocity

It was shown in the 2D solutions [4] that the pressure versus time dependence comprises two parts: the first is induced by the initial contact between the structure and the ice sheet, and the second one corresponds to structure penetration in the ice sheet. This result is confirmed in the 3D solution [10]. It was shown that the pressure time history consists of two parts: the amplitude of the first one is linearly proportional to ice velocity and the second only rather loose correlation with velocity. The pressure in the first part can be expressed as $P = \sqrt{\rho E U_0}$, which according to wave theory in solid materials exactly corresponds to pressure induced by hitting a wall by an elastic beam. The unloading wave arises due to influence of the sheet free surfaces. Therefore the duration of pressure in the first part is low and in full scale it can be omitted for wide structures.

The situation changes for very narrow structures especially if their natural period is comparable with duration of the high amplitude part of the pressure signal. Loads in that case can be high and they will increase with the increase in ice velocity. As the structure in narrow, the load will act about simultaneously over the whole contact surface. Several factors confirm this statement:

- increase of pressure on narrow pipe attached to ship bow with increase of ice velocity was registered in Kärnä et al. (1993);
- similar dependence is shown in Masterson and Frederking (1993) where pressures on the some area of ship bow is discussed;
- it is mentioned in several papers (e.g. [6]), that out of plane form of ice sheet edge after failure depends on ice velocity. The higher the velocity is, the more cracks are concentrated in a narrow zone near the structure.

It will be shown later (Fig. 3) that high pressure is distributed simultaneously and evenly along the contact area at high speeds. The pressure has a short duration time and therefore only a narrow layer of ice fails near the contact surface. This layer is extruded

79

with high velocity over a short time and again the structure meets about plane ice edge. The opposite is a failure process that develops gradually at low speed during penetration phase. It has time to cover great part of the ice sheet near the contact area and as it was shown in experiments by Sakai et al. (1999) and by numerical simulation by Kärnä et al. (2001) that two triangles form near the free surface and fly out.

Stress distribution over the contact area
The stress distribution depends on the ice velocity and ice properties.
Velocity:
If the ice sheet velocity is not very high the stress in an ice field after hitting the structure does not exceed the ice strength (with the present input data the critical velocity was about 0.4 m/s) and initially distributed evenly over the contact area. The stress at the corner as well as over the whole contact area gradually increases as the sheet displacement increases in the subsequent time (Fig. 4). If the velocity is high then initially pressure is distributed evenly as well, but this pressure leads to instant failure along the whole contact. The subsequent structure penetration in the ice induces stress increase but this loading develops through the destroyed layer (Fig. 4).
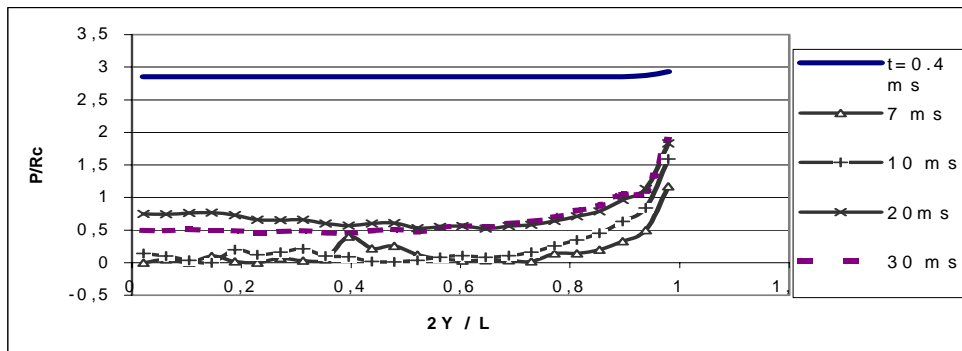

Fig. 3. Non-dimensional stress distribution along the central line of the contact area (axis Y) at different times t (ms). A relatively high ice velocity ($L = 20$m, $h = 4$ m, $U = 1$ m/s). Only the right part of the contact surface (with length $L/2$) is considered

If ice velocity is low then the evenly distributed pressure, induced by initial contact has the lowest level (Fig 4).

Plasticity
It is well known that ice plasticity is linked to the strain rate, but the model described above does not take into account this dependence. Therefore it was decided to consider two independent models, namely about perfect plasticity which is close to the Treska and the modified Coulomb-Mohr criterion. The transitions to Treska were realised by use of the residual strength equal to 0.95 of the unconfined one and an angle of internal friction equal to 5° instead of 0.25 and 30° correspondingly in modified Coulomb-Mohr. Non-dimensional stress distribution over the contact surface in different time moment for "plastic" media is plotted in Fig. 4. It is seen that pressure is distributed evenly initially (during the initial contact) and then grows gradually as the structure penetrates the ice. As soon as a plastic limit is reached in some sheet section then

pressure over the next section (farther away from the structure corner) begins to grow and finally the whole surface besides the part near the corner is loaded evenly. The velocity of maximum pressure propagation along the contact surface depends on strain rate and significantly less than velocity of any elastic wave propagation in the ice. The final stress distribution in Fig. 4 is very similar to results that are obtained in experiments carried out by Takeuchi et al. (2001).
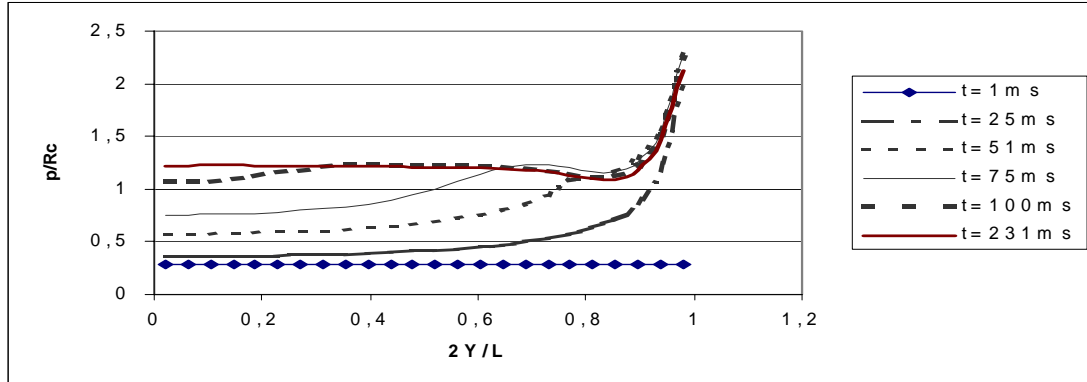

Fig. 4. Normal non-dimensional stress distribution along the central line of the contact area (axis Y)
in different time moments
(Plasticity , $L = 20$ m, $h = 1$ m, $U = 0.1$ m/s)

Stress concentration

The ratio of stress near the corner to maximal stress in the center of the structure is about 2, what is less than (2.5-4) in experiments by Takeuchi et al. (2001). Apparently this is a peculiarity for the plastic solution. The stress distribution near the corner absolutely does not depend on the structure length. Similar results were obtained for ice sheet thicknesses in the range of 1-4 m. In spite of relatively high level of stress concentration its input to effective pressure (when this pressure reaches maximum) does not exceed 4-5 %. So this concentration is more likely important for local loads than for global ones. It is important also that the maximum stress concentration and maximum effective pressure take place at different times.

Modified Coulomb-Mohr

(Parameters used in those experiments are listed in the beginning of the experiment results description). Pressure distribution over the contact surface at the initial stage of deformation (until failure beginning) in this case is similar to one in the foregoing simulation. The main difference starts with failure development in some point. When failure criterion is reached in some area, material after failure cannot resist very much to loading and as the structure penetration in ice (loading) continue to increase the maximum pressure is transferred to the neighbouring non damaged area, which can resist to loading. (Fig. 5).It can be seen in the figure that local maximal pressure moves along the contact surface with some velocity . It is interesting that this type of failure can form even in perfect conditions – absolutely homogeneous ice and plane contact.
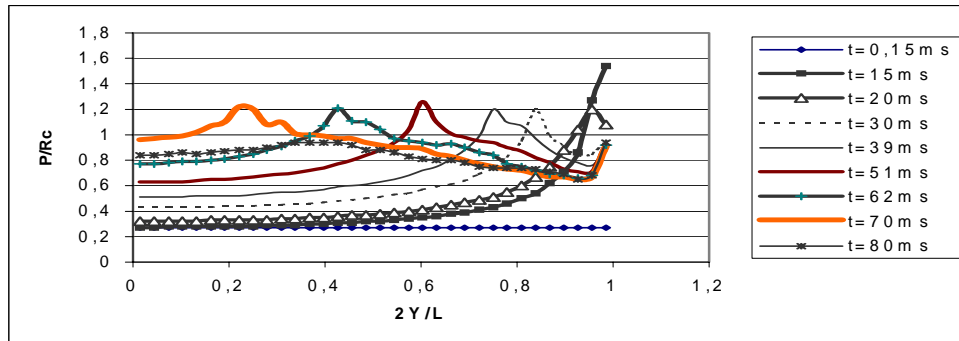
81

Fig. 5. Non dimensional stress distribution along the central line of the contact surface at different times.(L=20m, h=0.5m, V=0.1m/s)

Stress concentration:

Similarly to plasticity model the stress concentration appears near the corner. The ratio between the maximum stress in the corner to average effective stress varies in most of the experiments in the range 2-3. That is closer to the Takeuchi et al. (2001) experiments. The maximal local stresses in this case depend on ice sheet thickness. This dependence is approximately proportional to $h^{0.3}$. The area where the structure corner influences the pressure is approximately in the range of (0.5-1)·h.

Maximum effective pressure:

The maximal effective pressure P is determined as maximum of integral of instant pressures over the contact area. In spite of stress concentration near the corner, the *P* dependence on *h*, *L* and aspect ratio was very weak. Three factors can explain this result: it was not possible to consider aspect ratios less then 5; ice/structure friction effects were neglected and it was seen that the maximal stress concentration and maximal effective pressure take part at different times.

CONCLUSIONS

A 3D solution of level ice-structure interaction was developed and numerical experiments carried out. The major conclusions of the study are:

1. The effective pressure comprises two parts: One part relates to the first hit between structure and ice, the second part is connected to the structure penetrating the ice. The correlation between these parts depends mostly on the ice speed - the higher the speed, the more important the first part is. For the modulus of elasticity that is used in these experiments the firs part is predominant at U $\approx$ 0.5 m/s.
    At low speeds stresses increase gradually after the initial shock both for plastic and modified Coulomb-Mohr model. But depending on ice model the pattern is different when the failure criterion is reached. Maximal stresses distributed evenly over the contact area in plasticity and unevenly in the modified Coulomb-Mohr model.

2. The stress concentration near the corners may exceed significantly the pressure in other points of the contact surface. The level of concentration and area where corners influence the stress field depend on ice thickness. But the maximal effective pressure had low dependence on the ice thickness.

3. Qualitatively (and sometimes quantitatively) results of numerical experiments are in a good correlation with data obtained in experiments of Takeuchi et al. (2000, 2001).

REFERENCES

1. Frederking, R.M.W (1977): Plane strain compressive strength of columnar-grained and granular-snow ice. *Journal of Glaciology 18*(80), pp. 505–516.

2. Jilenkov,A., Kapustiansky, S., Shkhinek,K., Karna, T., Loset, S. (2002): 3D numerical simulation of ice sheet interaction with the wall. *In Proceedings of the IAHR Ice Symposium*, New Zealand, pp. 87-97.

3. Lysmer F. and Kuhlemeyer, R.L. (/1969): Finite dynamic model for infinite media. *ASCE 95*(11), pp. 859–877.

4. Kärnä, T., Shkhinek, K., Kapustiansky, S., Jilenkov, A., Määttänen, M. and Kolari, K. (2001): Ice-structure dynamics. *LOLEIF Report No. 8*, Hamburgische Schiffbau-Versuchsanstalt, 134 p.

5. Kärnä, T., Jarvinen, E., Nyman, T. And Viorio, J. (1993): Results from Indentation Tests in Sea Ice. *Proceedings of the OMAE Conference*, Glasgow, England, Vol.4, pp. 177-185.

6. Kärnä, T. (1994): Finite ice failure depth in penetration of a vertical indentor into an ice edge. *Annals of Glaciology 19*, pp. 114–120.

7. Masterson, D.M. and Frederking, R.M. (1993): Local Contact Pressures in Ship/Ice and Structure / Ice Interaction. *Cold Regions Science and Technology 21*, pp. 169-175.

8. Sakai M, Narita, K., Hamana Y., Takeuchi t., Saeki s., 1999. Experimental Study on Ice Sheet Strain Area According to Indentation Velocity in Field Indentation Tests. *Proceedings of the ISOPE Conference,* Vol. 2. pp. 512-516.

,9. Shkhinek, K., Kärnä, T., Kapustiansky, S. and Jilenkov, A. (1999): Numerical simulation of the ice failure process. *Proceedings of the 15th International Conference on Port and Ocean Engineering under Arctic Conditions (POAC)*, Vol. 2, pp. 877–887.

10. Shkhinek K., Loset S.&Karna T, 2003.Global ice loads dependency on structure width and ice thickness. *Proceedings of the POAC Conference*, pp. 857-867.

11. Schulson, E.M., Jones, D.E. and Kuehn, G.A. (1991): The effect of confinement on the brittle compressive fracture of ice. *Annals of Glaciology 15*, pp. 216–221.

12. Smith, T.R.and Schulson, E.M. (1993): The brittle compressive failure of fresh-water columnar ice under biaxial loading. *Acta metall. Mater. 41*(1), pp. 153–163.

13. Takeuchi, T., Kawamura, M., Sakai, M., Nakazawa, N.,et al. (2001): Ice loads equation by medium scale field indentation test data. *In Proceedings of the ISOPE Conference*, Vol. 1, pp. 713-720.

14. Wilkins, M.L., French, S. and Sorem, M. (1973): Finite-difference scheme for solving the 3D problems depending on time in the book (in Russian). Numerical methods in hydromechanics, pp. 115–119.